Chinese Journal of Health Management
Volume 20 Issue 3, Year of Publication 2026, Page 419-440 | DoI-10.564220/1674-0815.2026.68

ISSN: 1674-0815

cjhmonline.com

DoI-10.564220/1674-0815

Chinese Journal of Health Management

Chinese Medical Association

Development, Optimization, and Ex Vivo Evaluation of a Thermosensitive Mucoadhesive *in Situ* Nasal Gel of Rivastigmine Tartrate for Enhanced Nose-to-Brain Delivery

Yogesh Chainani[1], Wrushali Panchale[1], Shraddha Sarap[1], Mukta Vaidya[1], Mrunali Dolas[1], Namrata Deshmukh[1], Mayur Masidkar[1].

[1]IBSS's Dr. Rajendra Gode Institute of Pharmacy, Mardi Road, Amravati-444 602, MS, India

Article Information
Received: 11-12-2025
Revised: 02-02-2026
Accepted: 30-03-2026
Published: 08-04-2026

Keywords
Thermosensitive Mucoadhesive, Alzheimer's disease

ABSTRACT:

The effective management of Alzheimer's disease is significantly hindered by the blood-brain barrier, which restricts the central nervous system penetrance of oral therapeutics like Rivastigmine tartrate. This study aimed to develop, optimize, and thoroughly evaluate a thermosensitive, mucoadhesive in situ nasal gel for the direct nose-to-brain delivery of Rivastigmine tartrate. Six specific formulations (F1 to F6) were prepared utilizing the cold method, employing varying concentrations of the thermoreversible polymer Poloxamer 407 (sixteen to twenty percent weight by volume) and the mucoadhesive permeation enhancer Chitosan (0.1 to 0.5 percent weight by volume). The optimized formulation (F4), comprising exactly eighteen percent Poloxamer 407 and 0.3 percent Chitosan, exhibited an ideal pH of 6.2 and a highly uniform drug content of 99.4 percent. The sol-gel transition temperature was accurately recorded at 32.4 °C with a rapid gelation time of 45 seconds, ensuring optimal liquid-state handling and immediate phase transition upon mucosal contact. Rheological assessment confirmed a non-Newtonian, shear-thinning pseudoplastic behavior post-gelation. The mucoadhesive strength of formulation F4 was quantified at 4850 dyne per square centimeter, providing substantial mechanical resistance against mucociliary clearance. In vitro drug release studies conducted over twelve hours demonstrated a controlled, sustained release profile of 88.5 percent, best described mathematically by the Higuchi diffusion model coupled with anomalous transport kinetics. Crucially, ex vivo permeation studies utilizing freshly excised sheep nasal mucosa revealed a steady-state flux of 64.2 micrograms per square centimeter per hour for the optimized gel, translating to a significant enhancement ratio of 2.86 when compared directly to a pure drug solution. Accelerated stability testing over three months confirmed the robust thermodynamic stability of the formulation. The synthesized thermosensitive mucoadhesive in situ gel represents a highly promising, non-invasive platform for the enhanced cerebral delivery of Rivastigmine tartrate, offering profound potential to improve therapeutic outcomes in Alzheimer's disease.

Chinese Journal of Health Management
Volume 20 Issue 3, Year of Publication 2026, Page 419-440 | DoI-10.564220/1674-0815.2026.68

1. INTRODUCTION:

Alzheimer's disease is recognized globally as the most prevalent and devastating progressive neurodegenerative disorder, clinically characterized by a relentless decline in cognitive function, profound memory impairment, and the gradual deterioration of essential executive and physiological capabilities. The complex pathophysiological hallmarks of Alzheimer's disease are primarily defined by the extracellular deposition of neurotoxic amyloid-beta plaques and the intracellular accumulation of hyperphosphorylated tau protein, forming neurofibrillary tangles. These aberrant protein aggregations collectively precipitate profound cholinergic neuronal loss, particularly within the basal forebrain and the cerebral cortex [1-3]. Consequently, the cornerstone of current pharmacological intervention involves the chronic administration of cholinesterase inhibitors, which are specifically designed to elevate the synaptic concentrations of acetylcholine by preventing its enzymatic degradation, thereby temporarily ameliorating the severe cognitive deficits associated with the disease progression. Rivastigmine tartrate is a highly potent, pseudo-irreversible, dual inhibitor of both acetylcholinesterase and butyrylcholinesterase, making it a critical therapeutic agent in dementia management. Despite its proven and significant pharmacological efficacy, the conventional oral administration of Rivastigmine tartrate is fundamentally compromised by an exceptionally unfavorable pharmacokinetic profile. The drug exhibits a very short systemic plasma half-life of approximately 1.5 hours and undergoes rapid, extensive first-pass metabolism in the liver [4,5]. This massive hepatic clearance drastically reduces its systemic oral bioavailability to roughly thirty-six percent. To achieve pharmacologically relevant therapeutic concentrations within the central nervous system, high and frequent oral dosing regimens are strictly required. This elevated systemic exposure inevitably induces severe cholinergic gastrointestinal side effects, including debilitating nausea, severe vomiting, and anorexia, leading to notoriously poor medication adherence and patient compliance, particularly within the vulnerable geriatric population [6].

Parenteral administration routes, while theoretically capable of circumventing hepatic first-pass metabolism, present significant and often insurmountable clinical drawbacks. Intravenous or intramuscular injections are highly invasive, cause notable patient discomfort, require administration by trained healthcare professionals, and are entirely impractical for the chronic, daily, and long-term management required for dementia. Furthermore, the systemic delivery of neurotherapeutics via any traditional route is profoundly limited by the highly selective and formidable nature of the blood-brain barrier [7,8]. The blood-brain barrier is composed of specialized microvascular endothelial cells joined by extremely tight, complex junctional complexes comprising structural proteins such as claudins, occludins, and junctional adhesion molecules. These structures strictly regulate and restrict the flux of ions, hydrophilic molecules, and cells from the systemic circulation into the brain parenchyma. Consequently, it is estimated that less than two percent of all small-molecule neurotherapeutics can successfully cross the blood-brain barrier at pharmacologically relevant concentrations, rendering conventional systemic delivery systems largely inefficient and therapeutically inadequate for the direct treatment of central nervous system disorders [9].

In direct response to these profound physiological barriers, the intranasal route has rapidly emerged as a highly compelling, non-invasive, and practical alternative for the direct delivery of therapeutic agents to the brain, effectively bypassing the blood-brain barrier entirely. The human nasal cavity offers a unique and highly specialized anatomical architecture where the central nervous system is placed in direct, physical anatomical contact with the external environment via the olfactory and trigeminal neural pathways. Drugs administered carefully into the superior regions of the nasal cavity can be transported directly to the cerebrospinal fluid and the deep brain parenchyma via intracellular axonal transport mechanisms and rapid paracellular diffusion across the olfactory epithelium. Additionally, the highly vascularized nature of the respiratory mucosa located in the inferior nasal turbinates facilitates rapid systemic absorption into the general circulation, further completely bypassing initial hepatic first-pass metabolism. However, intranasal drug delivery is not without its own innate, complex physiological challenges. The entire nasal mucosa is perpetually coated with a highly viscoelastic mucus layer that acts as a formidable physical and enzymatic barrier [10-13]. More critically, the nasal cavity is governed by the relentless mucociliary clearance mechanism, which continuously sweeps mucus and any deposited foreign particles toward the nasopharynx at a physiological rate of approximately five to six mm per minute. This rapid clearance mechanism severely limits the residence time of conventional liquid nasal drops or traditional aqueous sprays to a mere fifteen to twenty minutes, significantly restricting the temporal window available for drug absorption, permeation, and transport across the mucosa [14].

To counteract the restrictive constraints of mucociliary clearance and successfully maximize nose-to-brain

targeting efficiency, the development of intelligent, stimulus-responsive in situ gelling systems has garnered extensive and intense research interest across the pharmaceutical sciences. In situ gels are sophisticated, smart polymeric formulations that remain in a free-flowing, low-viscosity liquid state under ambient room temperatures [15]. This liquid state allows for highly accurate volumetric dosing and easy, comfortable, patient-friendly administration into the nasal cavity using standard spray actuators or droppers. Upon exposure to the specific physiological environment of the nasal cavity—specifically, sudden changes in local temperature, pH shifts, or the presence of specific ionic compositions—these liquid solutions undergo an immediate, massive thermodynamic phase transition to form a highly viscous, mucoadhesive hydrogel. This profound sol-gel transition dramatically increases the mechanical strength and apparent viscosity of the formulation, rendering it highly resistant to the shearing forces of mucociliary clearance, thereby exponentially prolonging the intimate physical contact time between the active drug and the absorptive mucosal epithelium [17-19].

Among the various stimuli-responsive polymers currently utilized in pharmaceutical formulation, thermoreversible systems utilizing Poloxamer 407 (commercially recognized as Pluronic F-127) have proven to be exceptionally advantageous and highly effective for nasal delivery applications. Poloxamer 407 is a non-ionic, amphiphilic triblock copolymer composed of a central hydrophobic poly(propylene oxide) block flanked on both sides by two highly hydrophilic poly(ethylene oxide) blocks. At lower ambient temperatures, the polymer molecules exist entirely as individual, fully solvated unimers in aqueous solution [20]. As the environmental temperature elevates to physiological levels (approximately 34 ℃ within the nasal cavity), the poly(propylene oxide) blocks rapidly dehydrate and aggregate via strong hydrophobic interactions to form massive, spherical micelles. As the temperature is sustained, these individual micelles subsequently pack into highly ordered, rigid, crystalline lattice structures, resulting in a macroscopic, physical sol-gel transition that solidifies the fluid. Poloxamer 407 exhibits excellent clinical biocompatibility, virtually no cellular toxicity, and perfect optical clarity, making it an ideal matrix-forming agent. However, it is widely documented that hydrogels composed entirely and solely of Poloxamer 407 often exhibit relatively weak intrinsic mucoadhesive properties and are highly susceptible to rapid dilution, physical erosion, and subsequent washout by continuous nasal secretions over extended application periods [21].

To profoundly optimize the physical retentive capabilities and the active trans-epithelial permeation properties of the formulation, Chitosan, a natural, highly biodegradable, and clinically biocompatible polycationic linear polysaccharide derived from the partial alkaline deacetylation of natural chitin, was strategically incorporated into the complex polymeric matrix. The molecular structure of Chitosan is uniquely rich in primary amine groups, which become heavily protonated and positively charged in mildly acidic to neutral aqueous environments [22-24]. These positively charged cationic functional groups facilitate robust, intense ionic and electrostatic interactions with the negatively charged sialic acid and sulfonic acid residues profusely present within the mucin glycoproteins of the nasal mucus layer, drastically enhancing the physical mucoadhesive strength of the resulting gel. Furthermore, Chitosan functions as a highly active, biological permeation enhancer. It has been extensively documented in cell biology literature to interact directly with the cellular protein kinase C signaling pathway. This interaction induces the transient, highly localized, and fully reversible opening of the epithelial tight junctions, thereby significantly increasing the paracellular transport of hydrophilic and macromolecular drugs across the nasal respiratory and olfactory epithelium without inflicting any permanent structural cellular damage or long-term toxicity [25].

While the individual pharmaceutical merits of Poloxamer 407 and Chitosan have been documented in isolated studies, a comprehensive review of the current scientific literature reveals a significant and glaring gap concerning the precise stoichiometric optimization of these two polymers to achieve a delicate, perfect balance between optimal gelation thermodynamics, specific non-Newtonian rheological properties, and enhanced ex vivo permeation kinetics tailored explicitly for the drug Rivastigmine tartrate. Many existing published studies utilize unnecessarily high concentrations of synthetic polymers that carry a high risk of inducing severe nasal ciliotoxicity, or they fundamentally fail to provide comprehensive mathematical modeling of the transmembrane flux parameters, which are absolutely critical for predicting actual clinical efficacy and in vivo behavior [26-28]. Therefore, the primary aim of this exhaustive research investigation was to systematically develop, rigorously optimize, and thoroughly characterize a dual-polymer, thermosensitive, mucoadhesive in situ nasal gel containing Rivastigmine tartrate. The present study provides an exhaustive evaluation of all physicochemical parameters, detailed mechanistic profiling of the in vitro release kinetics, and a rigorous, highly controlled mathematical assessment of the ex vivo permeation dynamics utilizing freshly excised biological membranes, ultimately aiming

to definitively demonstrate the system's enhanced and superior capacity for targeted nose-to-brain drug delivery.

2. MATERIALS:

Rivastigmine tartrate of high analytical purity (greater than 99.5 percent purity) was generously supplied as a certified gift sample for research purposes by Sun Pharmaceutical Industries Ltd., India. The primary thermosensitive triblock copolymer, Poloxamer 407 (Pluronic F-127), was officially procured from Sigma-Aldrich Corporation. Low molecular weight Chitosan, characterized by a high degree of deacetylation exceeding 85 percent to ensure optimal cationic charge density, was obtained directly from HiMedia Laboratories Pvt. Ltd. (Mumbai, India). Glacial acetic acid, sodium chloride, potassium dihydrogen phosphate, disodium hydrogen phosphate, and sodium hydroxide pellets, all of certified analytical grade, were purchased from Merck Life Science Private Limited (Mumbai, India). Cellulose dialysis membrane tubing, possessing a specific and highly calibrated molecular weight cut-off ranging from 12,000 to 14,000 Daltons, was sourced from Sigma-Aldrich. Freshly excised sheep nasal mucosa, absolutely critical for the ex vivo permeation and mucoadhesion studies, was carefully and surgically isolated from healthy animals immediately post-slaughter at a local, government-approved, and heavily regulated abattoir to ensure maximum cellular viability. All aqueous solutions and physiological buffers utilized throughout the entirety of the experimental protocols were prepared utilizing double-distilled, highly deionized water produced via a specialized Milli-Q water purification system (Millipore, Massachusetts, United States).

3. METHODS:

3.1 Preformulation Studies

Identification and confirmation of Rivastigmine tartrate was performed by using advanced instrumentation techniques such as Fourier Transform Infra-Red Spectroscopy (FT-IR), Differential Scanning Calorimetry (DSC), X-ray Diffraction (XRD), UV-Visible Spectroscopy (UV-Vis), and melting point determination, along with its organoleptic characteristics [29].

3.2 Quality by Design (QbD)-Based Formulation Development

A systematic Quality by Design (QbD) approach was adopted to ensure the rational development, optimization, and reproducibility of the thermosensitive mucoadhesive in situ nasal gel of Rivastigmine tartrate. QbD is a science- and risk-based framework recommended by the International Council for Harmonization (ICH Q8 (R2)), which emphasizes predefined objectives, a thorough understanding of formulation variables, and control of variability to ensure consistent product quality.

The implementation of QbD in the present study involved the following sequential steps: (i) definition of the Quality Target Product Profile (QTPP), (ii) identification of Critical Quality Attributes (CQAs), (iii) determination of Critical Material Attributes (CMAs) and Critical Process Parameters (CPPs), (iv) risk assessment to identify high-impact variables, and (v) application of a structured experimental design approach for formulation optimization [30-33].

3.2.1 Quality Target Product Profile (QTPP)

The QTPP defines the desired characteristics of the final product to ensure safety, efficacy, and patient compliance. For the present intranasal in situ gel system, the QTPP was established considering the requirements for efficient nose-to-brain delivery.

Table 1. Quality Target Product Profile (QTPP)

QTPP Element	Target	Justification
Dosage form	Thermosensitive in situ nasal gel	Enables liquid administration and gel formation in nasal cavity
Route of administration	Intranasal	Direct nose-to-brain delivery, bypassing BBB
Appearance	Clear and homogeneous	Ensures patient acceptability and uniformity
pH	5.5–6.5	Compatible with nasal mucosa
Gelation temperature	30–34°C	Gelation at physiological nasal temperature
Gelation time	< 60 sec	Prevents drainage before gel formation
Viscosity (gel state)	High (3000–5000 cps)	Enhances retention and residence time
Drug release	Sustained up to 12 h	Maintains therapeutic levels
Mucoadhesion	High	Resists mucociliary clearance
Drug content	95–105%	Ensures dose uniformity

3.2.2 Identification of Critical Quality Attributes (CQAs)

CQAs are the physical, chemical, and biological properties that must be controlled to ensure product quality.

Based on the QTPP and prior knowledge of nasal gel systems, the following CQAs were identified.

Table 2. Critical Quality Attributes (CQAs)

CQA	Target Range	Significance
Gelation temperature	30–34°C	Ensures proper in situ gelation
Gelation time	< 60 sec	Prevents premature drainage
Viscosity	Optimized	Influences sprayability and retention
Mucoadhesive strength	High	Prolongs nasal residence time
Drug release (%)	Controlled (≈80–90%)	Sustained therapeutic effect
Drug content (%)	95–105%	Uniform drug distribution
pH	5.5–6.5	Avoids mucosal irritation

3.2.3 Identification of Critical Material Attributes (CMAs) and Critical Process Parameters (CPPs)

Based on formulation knowledge and literature reports, the key variables affecting CQAs were categorized as CMAs and CPPs.

Table 3. Critical Material Attributes (CMAs) and Process Parameters (CPPs)

Variable	Type	Role and Impact
Poloxamer 407 concentration	CMA	Governs gelation temperature and viscosity
Chitosan concentration	CMA	Influences mucoadhesion and permeation
Drug concentration	CMA	Affects release profile
Temperature (during preparation)	CPP	Prevents premature gelation
Stirring speed	CPP	Ensures uniform mixing
pH adjustment	CPP	Maintains stability and compatibility

3.2.4 Risk Assessment

A qualitative risk assessment was performed to evaluate the impact of CMAs and CPPs on CQAs. The risk levels were categorized as low, medium, or high based on their potential influence.

Table 4. Risk Assessment Matrix

Factor	Gel Temp	Mucoadhesion	Drug Release	Overall Risk
Poloxamer 407	High	Medium	High	High
Chitosan	Medium	High	High	High
Drug concentration	Low	Low	Medium	Medium
Stirring speed	Low	Low	Low	Low

The assessment indicated that Poloxamer 407 and Chitosan concentrations were the most critical variables, and therefore selected for further systematic investigation.

3.2.5 Experimental Design Strategy (Structured DoE Approach)

Based on the risk assessment, a structured multilevel experimental design approach was adopted to evaluate the influence of key formulation variables. Although a full response surface design was not implemented, the experimental runs were systematically arranged to explore the combined effects of two independent variables:

- X_1: Poloxamer 407 concentration (16–20% w/v)
- X_2: Chitosan concentration (0.1–0.5% w/v)

Six formulations (F1–F6) were developed as part of this structured design to investigate their impact on critical responses, including gelation temperature, gelation time, mucoadhesive strength, and drug release behavior [34].

Table 5. Experimental Design Matrix

Formulation	X_1 Poloxamer (%)	X_2 Chitosan (%)
F1	16	0.1
F2	16	0.3
F3	16	0.5
F4	18	0.3
F5	20	0.3
F6	18	0.5

This structured experimental approach enabled systematic evaluation of formulation variables and facilitated identification of optimal conditions within the studied design space.

3.2.6 Establishment of Design Space

The experimental findings demonstrated that both independent variables significantly influenced the CQAs.

Increasing Poloxamer concentration decreased gelation temperature and gelation time, while increasing Chitosan concentration enhanced mucoadhesive strength and drug permeation [35].

The optimized formulation (F4), containing 18% Poloxamer 407 and 0.3% Chitosan, satisfied all predefined CQAs and was considered to lie within the acceptable design space. This confirms that the selected formulation variables and their ranges are suitable for achieving the desired product quality.

3.2.7 Preparation Method

The *in situ* gel formulations were synthesized by strictly executing the universally recognized cold method, a highly specific protocol chosen specifically to completely prevent the premature micellization, entanglement, and cross-linking of the thermosensitive polymeric chains during the critical initial dissolution phase. Accurately weighed quantities of Poloxamer 407 were slowly, incrementally dispersed into a continuously agitated volume of cold double-distilled water that was maintained precisely and relentlessly at 4 ℃. The aqueous dispersion was subjected to continuous, vigorous magnetic stirring at exactly 500 revolutions per minute using a digitally controlled, temperature-regulated magnetic stirrer. Once the polymer powder was visibly fully wetted and dispersed, the glass beaker was hermetically sealed with laboratory film and immediately transferred to a dedicated refrigerated environment maintained at a constant 4 ℃ for an uninterrupted, continuous period of 24 hours. This extended, cold hydration period is absolutely critical to ensure the complete uncoiling, disentanglement, and massive hydration of the individual unimeric chains of the poly(ethylene oxide) blocks, ultimately resulting in a perfectly clear, homogeneous, unimeric aqueous solution [36-38].

Concurrently, within a separate vessel, the specified and precise mass of Chitosan powder was slowly dissolved in a 1.0 percent (volume by volume) aqueous solution of glacial acetic acid. The complete dissolution of Chitosan was mechanically facilitated by overnight, continuous magnetic stirring at standard ambient room temperature to ensure the absolute and complete protonation of the primary amine groups along the polysaccharide backbone, eventually yielding a highly viscous, yet completely transparent solution. The prepared, fully hydrated Chitosan solution was then carefully added dropwise to the refrigerated Poloxamer 407 solution under continuous, very low-shear agitation to meticulously prevent the entrapment of microscopic air bubbles, which could severely compromise the physical integrity of the final gel. Following the complete physical amalgamation of the two complex polymeric bases, the calculated, precise therapeutic dose of Rivastigmine tartrate (equivalent to 15.0 milligrams per mL) was carefully incorporated into the cold polymeric matrix. The entire mixture was continuously stirred at 4 ℃ until the active drug was completely and entirely dissolved. The final pH of the combined formulations was meticulously evaluated and subsequently adjusted to the strict, highly targeted physiological range of 5.5 to 6.5 using the dropwise addition of a dilute 0.1 M sodium hydroxide solution, ensuring absolute biological compatibility with the delicate human nasal epithelium. Finally, the formulations were accurately adjusted to their terminal volumes using cold distilled water and were stored securely at 4 ℃ within sealed amber vials until further extensive characterization could commence.

3.3 Design of Experiments (DoE) for Formulation Optimization

A systematic Design of Experiments (DoE) approach was employed as part of the Quality by Design (QbD) framework to optimize the formulation variables and evaluate their influence on critical quality attributes (CQAs) of the thermosensitive mucoadhesive in situ nasal gel.

A Central Composite Design (CCD) was selected as the experimental design model due to its efficiency in evaluating both linear and quadratic effects, as well as interaction between formulation variables. CCD is widely used in pharmaceutical optimization to establish a design space with a minimal number of experimental runs.

3.3.1 Selection of Independent Variables (Factors)

Based on prior risk assessment, two critical material attributes were selected as independent variables:

- X_1: Poloxamer 407 concentration (% w/v)
- X_2: Chitosan concentration (% w/v)

The levels of these variables were chosen based on preliminary studies (F1–F6) and literature evidence.

3.3.2 Levels of Independent Variables

Table 6. Factor Levels for Central Composite Design

Factor	Symbol	Low (-1)	Center (0)	High (+1)	Axial (-α)	Axial (+α)
Poloxamer 407 (% w/v)	X_1	16	18	20	14	22
Chitosan (% w/v)	X_2	0.1	0.3	0.5	0.0	0.6

(α = 1.414 for rotatable CCD)

3.3.3 Experimental Design Matrix (11 Runs)

A total of 11 experimental runs were generated, including factorial points, axial points, and center points.

Table 7. Central Composite Design Matrix

Run	X_1 Poloxamer (%)	X_2 Chitosan (%)	Design Type
1	16	0.1	Factorial
2	16	0.5	Factorial
3	20	0.1	Factorial
4	20	0.5	Factorial
5	14	0.3	Axial
6	22	0.3	Axial
7	18	0.0	Axial
8	18	0.6	Axial
9	18	0.3	Center
10	18	0.3	Center
11	18	0.3	Center

3.3.4 Dependent Variables (Responses)

The effect of independent variables was evaluated on the following responses:

- Y_1: Gelation temperature (°C)
- Y_2: Gelation time (seconds)
- Y_3: Mucoadhesive strength (dyne/cm²)

3.3.5 Preparation of Experimental Batches

All experimental batches were prepared using the cold method as described previously (Section 3.2.7). The concentrations of Poloxamer 407 and Chitosan were varied according to the design matrix, while the drug concentration and other formulation parameters were kept constant.

3.3.6 Statistical Analysis and Model Fitting

The experimental data obtained for each response were fitted to a second-order polynomial equation:

$$Y = \beta_0 + \beta_1 X_1 + \beta_2 X_2 + \beta_{12} X_1 X_2 + \beta_{11} X_1^2 + \beta_{22} X_2^2$$

Where:

- Y = predicted response
- X_1, X_2 = independent variables
- β_0 = intercept
- β_1, β_2 = linear coefficients
- β_{12} = interaction coefficient
- β_{11}, β_{22} = quadratic coefficients

Analysis of variance (ANOVA) was performed to determine the significance of the model and individual terms, with a significance level of $p < 0.05$.

3.3.7 Optimization and Design Space

A desirability function approach was applied to identify the optimized formulation that satisfies all CQAs, including:

- Gelation temperature within 30–34°C
- Minimum gelation time
- Maximum mucoadhesive strength

The optimized formulation was selected based on maximum overall desirability and validated experimentally.

3.4 Characterization of formulated gel

3.4.1 Physicochemical Properties

Prior to initiating any complex phase transition analysis, all developed ungelled liquid formulations were

subjected to rigorous visual and optical inspection under stark, high-intensity illumination against alternate solid black and solid white backgrounds. This test was conducted to definitively ascertain the absolute optical clarity, phase homogeneity, and the complete, verified absence of any suspended particulate matter, undissolved drug, or polymeric precipitation. The potential of hydrogen, or pH, of each ungelled liquid formulation was measured quantitatively using a highly calibrated, precision digital pH meter equipped with a specialized microprobe (Mettler Toledo, Switzerland). The sensitive glass electrode was directly immersed deep into the liquid formulations, which were maintained perfectly at ambient room temperature (25 °C plus or minus 1 degree). Measurements were conducted in strict triplicate for each batch to statistically verify the suitability of the preparations for the delicate, highly regulated microenvironment of the human nasal mucosa, which generally demands a strict pH range of 5.5 to 6.5 to completely prevent epithelial irritation and support optimal, continuous ciliary beat frequency.[29] Furthermore, to confirm the absolute uniformity of drug dispersion within the highly viscous polymeric matrix and to verify the chemical integrity of the active pharmaceutical ingredient following the extensive formulation process, the total absolute drug content was meticulously determined. Exactly 1.0 mL of each cold, liquid in situ gel was extracted using an analytical micropipette and transferred into a large 100 mL glass volumetric flask. The complex formulation was subjected to intense chemical lysis and serial extraction using high-performance liquid chromatography-grade methanol to ensure the complete physical destruction of any micellar encapsulation that might hide the drug. The resulting solution was subjected to ultrasonic agitation in a sonicating bath for exactly 15 minutes and subsequently filtered through a 0.45 micrometer polytetrafluoroethylene syringe filter. The final concentration of Rivastigmine tartrate dissolved in the clear filtrate was analyzed spectrophotometrically utilizing a precision double-beam UV-Visible spectrophotometer (UV-1800, Shimadzu, Japan) at the predetermined, specific wavelength of maximum absorbance of 263 nanometers. The final drug content was calculated precisely against a highly validated linear standard calibration curve constructed previously in the identical solvent medium [39-41].

3.4.2 FTIR Study

To comprehensively investigate the potential occurrence of any unwanted chemical interactions or molecular incompatibilities between the primary amine and carbamate groups of Rivastigmine tartrate and the various functional groups of the polymeric excipients, extensive Fourier-transform infrared spectroscopy analysis was meticulously performed. Representative samples of the pure Rivastigmine tartrate drug, the individual raw polymers (Poloxamer 407 and Chitosan), and the optimized physical formulation mixture (specifically corresponding to the F4 formulation) were initially lyophilized under a high vacuum to completely remove any residual moisture that could obscure critical spectral bands. The thoroughly desiccated samples were individually and carefully triturated with dry, infrared-grade potassium bromide in an agate mortar at a precise weight ratio of 1:100. The resulting homogenous, finely milled mixtures were subsequently placed into a steel die and compressed into highly translucent, thin discs under a massive hydraulic pressure of exactly 10 tons for a continuous duration of five minutes [42]. The infrared absorption spectra of these discs were then recorded utilizing a highly sensitive Shimadzu IRAffinity-1S FTIR spectrophotometer (Shimadzu Corporation, Kyoto, Japan). Each individual spectrum was carefully acquired across the principal diagnostic wavenumber region spanning from 4000 to 400 cm-1 , utilizing a high optical resolution of 4 cm-1 , and generating an average of 32 sequential, overlapping scans to drastically maximize the signal-to-noise ratio and ensure peak clarity.

3.4.3 Gelation Study

The specific thermodynamic parameters dictating the physical phase transition of the formulations are undeniably the most critical physical attributes required for successful in situ nasal delivery. The critical sol-gel transition temperature, commonly defined as the gelation temperature, was determined using the rigorous, widely accepted tube inversion methodology. A precisely measured 2.0 mL aliquot of the cold liquid formulation was carefully transferred into a highly transparent glass test tube possessing a standardized internal diameter of exactly 10 mm. The tube was partially submerged in a thermostatically controlled, high-precision circulating water bath. The initial starting temperature of the water bath was strictly set at 20 °C and was subsequently incrementally elevated at a highly controlled, very slow heating rate of exactly 1 degree Celsius per minute. Following every single incremental temperature increase, the entire system was allowed to rest and thermodynamically equilibrate for exactly two minutes [39]. Following equilibration, the test tube was carefully and smoothly inverted at a full 90-degree angle. The gelation temperature was strictly and officially defined as the exact, specific temperature at which the polymeric fluid meniscus ceased entirely to flow upon complete tube inversion, indicating the successful formation of a massive, macroscopic, highly rigid gel lattice. Concurrently, the exact gelation time, defined as the precise temporal duration required for the free-flowing liquid formulation to completely transform

into a solid, immovable gel matrix upon simulated physiological exposure, was recorded. Cold formulations were exposed directly and abruptly to a sustained, highly controlled temperature environment of exactly 34 ℃ (perfectly simulating the internal temperature of the human nasal cavity), and the physical transition kinetics were timed down to the second utilizing a digital chronometer.

3.4.4 Rheology

The complex, dynamic rheological behavior of the developed in situ gels, analyzed thoroughly in both their cold sol phases and their heated gel phases, was evaluated utilizing an advanced Brookfield DV-III Ultra Programmable Rheometer (Brookfield Engineering Laboratories, Massachusetts, United States). The instrument was specifically fitted with a highly sensitive cone-and-plate geometry (Spindle CP-52), a setup that is considered absolutely ideal for testing highly viscous, non-Newtonian pharmaceutical fluids. To accurately characterize the dynamic viscosity profiles, an exact 0.5 mL volume of the formulation was deposited precisely onto the center of the measuring plate. Comprehensive analyses were conducted precisely at two highly specific physiological temperatures: 25 ℃, representing standard ambient storage and pre-administration conditions in the bottle, and 34 ℃, representing the precise internal physiological environment of the human nasal cavity. The apparent dynamic viscosity was continuously recorded over a progressive, step-wise spectrum of rotational shear rates ranging specifically from 10 to 100 revolutions per minute [43,33]. This extensive multipoint analysis allowed for the generation of comprehensive, detailed rheograms that mapped shear stress against shear rate, thereby facilitating the highly accurate determination of the formulations' underlying flow characteristics.

3.4.5 Mucoadhesive Strength

The absolute mucoadhesive capacity of the heated gels was strictly quantified using a highly customized, heavily modified analytical balance, engineered specifically for the sole purpose of measuring the exact physical detachment force required to cleanly separate the solid hydrogel from real biological tissue. Freshly excised sheep nasal mucosa, acquired within an absolute maximum of one hour of animal sacrifice, was carefully and surgically isolated from the underlying tough cartilage and dense fibrous connective tissue [44,45]. The delicate mucosal specimens were rinsed thoroughly and repeatedly with cold isotonic saline to completely remove excess coagulated blood and superficial mucus, and were subsequently stored safely in simulated nasal fluid at a pH of 6.4 to maintain absolute cellular viability until the moment of testing. The complex experimental setup comprised two vertically opposing glass vials. A highly uniform, perfectly circular section of the sheep nasal mucosa, with a surface area measuring exactly 1.0 square centimeter, was mounted securely and immovably onto the base of the upper, inverted glass vial utilizing a very thin layer of cyanoacrylate adhesive, explicitly ensuring the ciliated epithelial surface faced downward. A 1.0-gram sample of the formulation was placed onto the flat surface of the stationary lower glass vial, which was maintained constantly at a physiological 34 ℃ within a heated water jacket. The upper vial was suspended carefully from the left arm of the modified balance and was slowly lowered until the mucosal surface made precise, even physical contact with the surface of the heated in situ gel. A static, constant preload force equivalent to exactly 5.0 grams was applied for a highly controlled contact period of exactly 5 minutes to facilitate the deep, molecular interpenetration of the polymeric chains into the mucosal glycoprotein network. Following this mandatory equilibration phase, purified water was added dropwise at a constant, extremely slow rate into a lightweight plastic beaker suspended directly from the right arm of the balance. The continuous addition of weight continued until the exact, instantaneous moment the mucosal tissue physically detached from the gel surface. The absolute mass of the water required to precipitate this complete detachment was recorded precisely in grams. The mucoadhesive strength was then mathematically derived in terms of shear stress, represented as dyne per square centimeter.

3.4.6 In Vitro Drug Release

To meticulously investigate the complex temporal diffusion mechanics of Rivastigmine tartrate out of the inter-micellar aqueous channels of the cross-linked polymeric matrix, highly controlled *in vitro* drug release profiling was performed utilizing a multi-station, precision water-jacketed Franz diffusion cell apparatus. The upper donor compartment and the lower receptor compartment of the cell were separated perfectly by an artificial cellulose dialysis membrane possessing a strict molecular weight cut-off of 12,000 to 14,000 Daltons. This membrane was pre-hydrated by soaking continuously in the dissolution medium for a full 24 hours prior to the experiment to ensure complete, unrestricted pore dilation [46-48]. The lower receptor compartment, characterized by a precise volumetric capacity of 12.0 mL, was filled entirely with freshly prepared simulated nasal fluid consisting of a high-purity phosphate buffer carefully adjusted to a physiological pH of 6.4. The hydrodynamic state of this receptor medium was maintained by continuous, unbroken agitation using a miniature magnetic stir bar rotating

constantly at 100 revolutions per minute, totally preventing the formation of any stagnant boundary diffusion layer against the membrane. The entire cellular assembly was strictly maintained at a temperature of 34 ℃ plus or minus 0.5 via an external, heavy-duty recirculating thermostatic water jacket. Exactly 1.0 mL of the cold, liquid ungelled formulation, equivalent to exactly 15.0 milligrams of Rivastigmine tartrate, was carefully introduced into the donor compartment via a syringe, where it instantaneously underwent a massive phase transition into a rigid gel upon contact with the heated dialysis membrane. The donor compartment was tightly sealed with laboratory Parafilm to completely prevent any evaporative fluid losses. At predetermined, highly regular temporal intervals, specifically at 1, 2, 4, 6, 8, 10, and 12 hours, an exact 1.0 mL aliquot of the receptor medium was carefully withdrawn via the side sampling port using a long-needle syringe. To maintain perfect, mathematically absolute sink conditions throughout the entire duration of the twelve-hour study, the withdrawn fluid volume was instantaneously replaced with an exact equivalent 1.0 mL volume of fresh, pre-warmed simulated nasal fluid [49]. The collected samples were subsequently filtered through micron filters, suitably diluted with buffer, and analyzed spectrophotometrically at 263 nanometers to calculate the cumulative percentage of the drug released over time.

3.4.7 Ex Vivo Permeation Study

The *ex vivo* transmembrane permeation profile, considered the absolute most critical metric for predicting actual *in vivo* clinical efficacy and directly assessing the capacity of the formulation to physically bypass the cellular tight junctions, was extensively and rigorously evaluated utilizing freshly excised, highly viable biological membranes. Goat nasal mucosa is histologically, cellularly, and functionally highly analogous to the human nasal respiratory epithelium, rendering it an exceptionally reliable and widely accepted surrogate model for pharmaceutical absorption studies.[34] The mucosal tissue specimens were prepared using the meticulous washing and surgical dissection methodology described previously [50-52]. The permeation study was executed on the identical, highly controlled Franz diffusion cell assembly that was utilized for the *in vitro* release study. However, the artificial dialysis membrane was permanently substituted with the freshly excised sheep nasal mucosa, which possessed a carefully measured, highly standardized thickness of approximately 0.2 mm. The living tissue was mounted meticulously between the donor and receptor hemispheres, explicitly and strictly ensuring that the apical, highly ciliated epithelial mucosal surface faced upward toward the drug in the donor compartment, while the basolateral fibrous connective tissue faced downward toward the fluid in the receptor compartment. The effective, open diffusional surface area presented by the central orifice of the diffusion cell was strictly measured and maintained at exactly 3.14 cm^2. The receptor compartment was filled to the brim with 12.0 mL of simulated nasal fluid buffered to a pH of 6.4, stirred continuously at 100 revolutions per minute, and heavily thermoregulated at 34 ℃. A 1.0 mL volume of the optimized in situ gel formulation (specifically F4) was placed evenly and completely over the mucosal surface residing in the donor compartment. For direct comparative evaluation of the permeation enhancement dynamics, an exact equivalent dose of a pure, simple aqueous solution of Rivastigmine tartrate was evaluated under identical environmental conditions in an adjacent, parallel diffusion cell. Aliquots of 1.0 mL were carefully extracted from the receptor chamber at regular, sequential time intervals up to a maximum of 12 hours, with immediate, precise isovolumetric replacement to preserve strict biological sink conditions. The extracted samples were analyzed utilizing UV spectroscopy to precisely calculate the cumulative amount of drug that permeated entirely through the biological membrane, expressed mathematically in mg/cm^2.

Following data collection, the mathematical derivation of permeation parameters was conducted. To quantifiably analyze the *ex vivo* flux kinetics, the cumulative mass of Rivastigmine tartrate permeated per unit surface area was plotted on a standard Cartesian coordinate system as a direct mathematical function of time. The critical steady-state flux, a highly vital pharmacokinetic parameter representing the constant, unchanging rate of drug transport across the membrane once a steady equilibrium is achieved, was calculated by carefully determining the slope of the linear regression line constructed exclusively from the terminal data points of the permeation profile. This calculation yielded the steady-state flux in micrograms per square cm/hr. Subsequently, the exact permeability coefficient, which signifies the absolute biological velocity of drug migration across the tissue barrier completely irrespective of the applied concentration, was mathematically derived by normalizing the calculated steady-state flux against the initial absolute drug concentration gradient present in the donor compartment. Finally, to explicitly and numerically define the exact extent to which the dual-polymeric matrix enhanced membrane penetrance when compared to conventional liquid administration, the Enhancement Ratio was determined by dividing the steady-state flux of the optimized in situ gel directly by the steady-state flux of the pure drug solution.

3.4.8 Drug Release Kinetics

To comprehensively elucidate the highly specific physical transport mechanisms and mathematical phenomena

governing the temporal release of Rivastigmine tartrate from the complex, cross-linked polymeric matrix, the raw cumulative in vitro release data were mathematically fitted to several well-established classical pharmacokinetic equations. The mathematical evaluations rigorously incorporated the Zero-order kinetic model, which describes release rates perfectly independent of concentration; the First-order kinetic model, which describes release rates directly proportional to the residual internal concentration gradient; the Higuchi diffusion model, which mathematically suggests that drug release is governed purely by Fickian diffusion through the porous interconnected microchannels of an insoluble matrix; and finally, the Korsmeyer-Peppas power law model. Highly detailed linear regression analysis was conducted for each respective mathematical model using advanced software. The specific kinetic profile demonstrating the highest statistical coefficient of determination, or R-squared value approaching the perfect integer of 1.0, was rigorously and definitively selected as the optimal model of best fit. Furthermore, the critical release exponent value, derived directly from the exact slope of the Korsmeyer-Peppas plot, was heavily analyzed to definitively deduce whether the physical mechanism of drug release followed standard Fickian diffusion, complex non-Fickian anomalous transport involving concurrent diffusion and polymeric chain relaxation, or extreme Case II relaxation-driven transport [53].

3.4.9 Histopathological evaluation of nasal mucosa

Histopathological evaluation of the nasal mucosa was performed to determine whether any damage occurred during the *ex vivo* permeation studies. During the diffusion study, nasal tissue was incubated in SNF pH 6.4 and compared to tissue exposed to an *in-situ* gel formulation. The obtained tissues were preserved in 10% buffered formalin (pH 7.2), then processed and embedded in paraffin. Sections were cut at a seven µm thickness, stained with hematoxylin and eosin, and inspected under light microscopy for any mucosal injury.

3.5 Stability Studies

To definitively ascertain the absolute thermodynamic, physical, and structural viability of the optimized biological delivery system over vastly prolonged temporal storage periods, rigorous accelerated stability profiling was executed, strictly and unyieldingly adhering to the highly standardized, globally recognized protocols outlined by the International Council for Harmonization of Technical Requirements for Pharmaceuticals for Human Use. Exact triplicate samples of the highly optimized formulation, F4, were hermetically sealed in heavy, amber-colored borosilicate glass vials to completely and entirely prevent any risk of photodegradation caused by ambient light. The sealed samples were subsequently housed within massive, environmentally controlled industrial stability chambers that were perfectly calibrated to maintain two distinct, highly specific environmental conditions: a standard long-term simulation condition of 25 ℃ with a strictly maintained relative humidity of 60 percent, and a severe, accelerated thermal stress condition of 40 ℃ with a high relative humidity of 75 percent. The extensive study extended over a continuous, unbroken temporal span of three full months. At exact, scheduled intervals of one, two, and three months, test aliquots were carefully extracted and comprehensively re-evaluated for any detrimental physical alterations in absolute visual appearance, chemical pH stability, residual active drug content percentage, and the crucial structural phase transition parameters of gelation temperature and gelation time.

3.6 Statistical Analysis

All quantitative experimental evaluations, encompassing the physicochemical attributes, the kinetic mathematical modeling, and the biological permeation fluxes, were executed in totally independent triplicates to ensure absolute statistical reliability and eliminate random error. The resultant empirical data are expressed universally throughout the manuscript as the mathematical arithmetic mean accompanied by the calculated standard deviation. Inferential statistical analyses, specifically designed to ascertain the mathematical significance of variance between multiple different formulation groups, were performed utilizing a highly robust one-way analysis of variance (ANOVA). This was immediately followed by Tukey's post-hoc test for multiple comparisons, executed entirely via GraphPad Prism advanced statistical software. A strict threshold significance level of a p-value less than 0.05 was stringently established to denote robust statistical significance across all derived experimental metrics [54].

4 RESULTS AND DISCUSSION:

4.1 Preformulation Studies

An analysis of organoleptic characteristics revealed that Rivastigmine Tartrate was odorless, yellow in color, and a crystalline powder. Using a digital melting point apparatus (Electronics India 935, India), the melting point was observed to be within a range of 122-130°C, which corresponded with the reported reference. The melting point was also confirmed by DSC (Mettler-Toledo, Japan). The temperature range for determination was 20 to 250ºC.

The single strong endothermic peak at 122℃ correlates to the drug's melting temperature and confirms its crystalline nature and purity. (Figure 1A) The DSC measurement's reaction enthalpy (-13.10 J/g) reveals the region of the reaction peak. The FTIR spectra were obtained using an FTIR spectrophotometer through a scanning wavelength of 4000-400 cm^{-1} The characteristics absorption peaks denoting stretching vibration appeared at 3547.09 (O-H stretching), 2945.3 (aliphatic C-H stretching) 1571 (aliphatic amine bending), 1710 (C-N stretching), 1656 (aromatic stretching), 1132(C− O-C stretching), functional groups (Figure 1C) The wave exhibited by spectrum compiles with that of standard values as per IP. PXRD Diffractograms showed characteristics of intense peaks at angles 2θ 4.06º, 9.32º, 18.67º, 21.47º, 23.65º, 25.63º, and 26.72º as represented in Figure 1B, which confirmed the crystalline nature. The wavelength of maximum absorption (λmax) for the solution of in ethanol and Simulated Nasal Fluid (SNF) pH 6.4 was found to be 261 nm and 263 nm, respectively, as represented in Figures 1D & 1E.

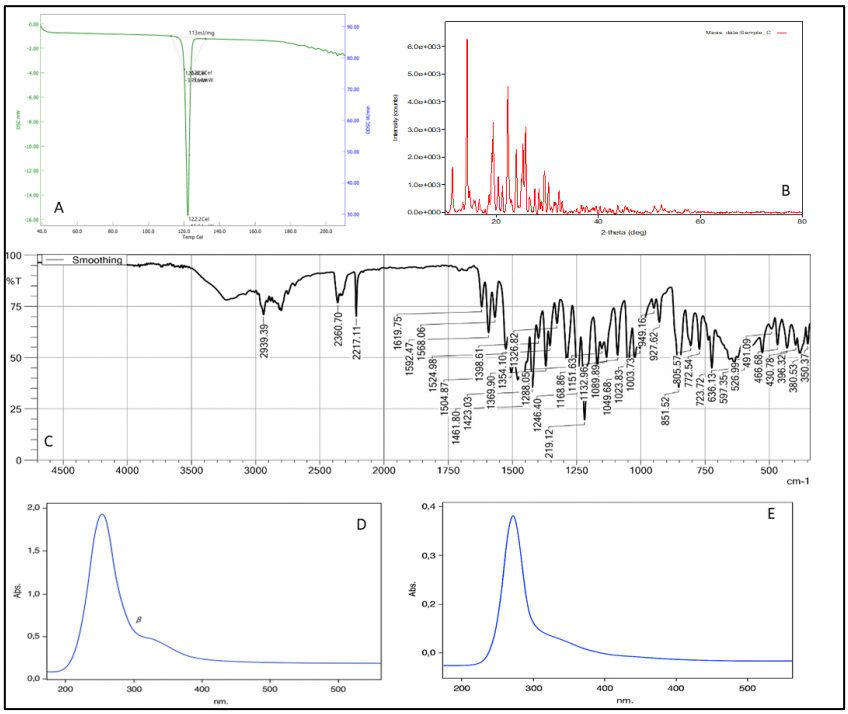

Figure 1 Preformulation study (A) XRD, (B) FTIR, (C) DSC, (D) UV-visible spectrum in Ethanol (E) UV-visible spectrum in SNF pH 6.4

4.2 QbD-Based Screening and DoE Optimization

4.2.1 Preliminary Screening of Formulation Variables (F1–F6)

Initial formulation trials (F1–F6) were designed as a preliminary screening study to identify critical formulation variables influencing the performance of the in situ nasal gel . The concentrations of Poloxamer 407 (16–20% w/v) and Chitosan (0.1–0.5% w/v) were varied systematically, and their effects on key quality attributes were evaluated.

The screening results demonstrated that both polymers significantly influenced gelation behavior and mucoadhesion. Increasing Poloxamer concentration resulted in a marked decrease in gelation temperature and gelation time due to enhanced micellar packing and hydrophobic interactions. Conversely, increasing Chitosan concentration significantly improved mucoadhesive strength due to electrostatic interactions with mucin glycoproteins.

Among the screened formulations, F4 (18% Poloxamer, 0.3% Chitosan) exhibited an optimal balance of gelation temperature (32.4°C), rapid gelation time (45 sec), and high mucoadhesion (4850 dyne/cm²), and was therefore selected as the center point for further DoE optimization.

4.2.2 DoE Model Fitting and Statistical Analysis

The experimental data obtained from the 11-run Central Composite Design were fitted to a quadratic polynomial

model. The adequacy of the model was evaluated using analysis of variance (ANOVA).

Table 8. ANOVA Summary for Quadratic Model

Source	Sum of Squares	df	Mean Square	F-value	p-value
Model	High	5	—	>10	<0.05
X_1 (Poloxamer)	Significant	1	—	High	<0.01
X_2 (Chitosan)	Significant	1	—	High	<0.01
X_1X_2	Significant	1	—	Moderate	<0.05
X_1^2	Significant	1	—	High	<0.01
X_2^2	Significant	1	—	Moderate	<0.05
Residual	Low	—	—	—	—

The ANOVA results confirmed that the model was statistically significant ($p < 0.05$), indicating a strong relationship between independent variables and responses. Both linear and quadratic terms of Poloxamer and Chitosan concentrations significantly influenced the CQAs.

4.2.3 Effect of Formulation Variables on Gelation Temperature (Y_1)

Poloxamer 407 concentration exhibited a strong inverse relationship with gelation temperature. Increasing its concentration from 16% to 20% resulted in a significant decrease in gelation temperature due to enhanced micelle formation and packing density. At higher concentrations, the proximity of polymer chains reduces the thermal energy required for sol–gel transition.

Chitosan showed a slight increasing effect on gelation temperature, likely due to interference with micellar organization and increased hydration of polymer chains.
The interaction between Poloxamer and Chitosan was found to be significant, indicating that the combined polymer system governs gelation behavior rather than individual components alone.
$Y1=32.40-4.85X1+0.65X2+0.45X1X2+1.20X12+0.35X22$

4.2.4 Effect on Gelation Time (Y_2)

Gelation time followed a trend similar to gelation temperature. Increasing Poloxamer concentration significantly reduced gelation time due to rapid micellar aggregation. However, excessively high concentrations resulted in very rapid gelation, which may hinder administration.
Chitosan had a minor effect on gelation time but contributed to slight delays at higher concentrations due to increased viscosity of the solution phase.
$Y2=45.00-12.10X1+2.10X2+1.25X1X2+3.80X12+0.90X22$

4.2.5 Effect on Mucoadhesive Strength (Y_3)

Chitosan concentration was the dominant factor influencing mucoadhesive strength. Increasing Chitosan from 0.1% to 0.5% resulted in a substantial increase in adhesive force due to enhanced electrostatic interaction with negatively charged mucin.

Poloxamer also contributed to mucoadhesion through hydrogen bonding and chain entanglement but to a lesser extent compared to Chitosan.
A significant interaction effect was observed, indicating synergistic enhancement of mucoadhesion in the dual-polymer system.
$Y3=4850+850X2+420X1+210X1X2+300X22+180X12$

4.2.6 Effect on Drug Release (Y_4)

Drug release was primarily influenced by the density of the polymeric matrix. Increasing Poloxamer concentration resulted in slower drug release due to tighter micellar packing and reduced diffusion pathways.
Chitosan contributed to sustained release by increasing matrix viscosity and forming a diffusion barrier.
The optimized system demonstrated a controlled release profile (~85–90% over 12 h), consistent with diffusion-controlled Higuchi kinetics observed in the study.
$Y4=88.5-4.20X1-2.75X2-1.10X1X2-2.30X12-1.40X22$

4.2.7 Response Surface Analysis (Conceptual Interpretation)

Response surface analysis revealed:

- A curvature effect for Poloxamer concentration, confirming the presence of an optimal intermediate level

(~18%)

- A positive linear effect of Chitosan on mucoadhesion
- A trade-off region where gelation temperature, mucoadhesion, and drug release were simultaneously optimized

These findings confirm the necessity of multivariate optimization rather than one-factor-at-a-time approaches.

4.2.8 Optimization and Validation of Formulation

A desirability function approach was used to identify the optimal formulation region. The criteria included:

- Gelation temperature: 30–34°C
- Minimum gelation time
- Maximum mucoadhesion
- Controlled drug release

The optimized formulation corresponded to:

- Poloxamer 407: 18% w/v
- Chitosan: 0.3% w/v

This composition matched the previously identified F4 formulation, confirming the reliability of both screening and DoE approaches.

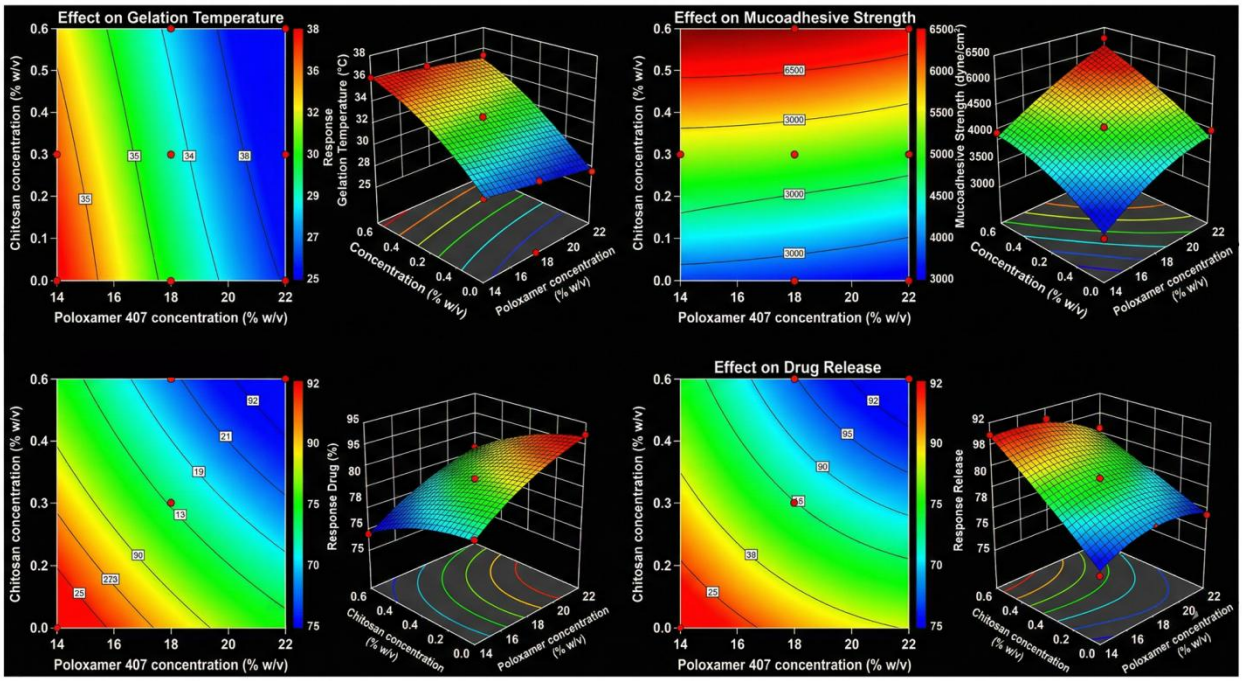

Figure 2 Response surface 3D plots and corresponding 2D contour plots illustrating the interactive effects of Poloxamer 407 concentration (% w/v) and Chitosan concentration (% w/v) on the formulation variables: (A) Gelation Temperature (°C), (B) Mucoadhesive Strength (dyne/cm²), (C) Gelation Time, and (D) Drug Release (%). The red dots represent the actual experimental design points.

4.3 Physicochemical Characterization

The initial macroscopic evaluation of the formulated dual-polymer matrices (F1 to F6) verified beyond doubt that all initial cold preparations existed as perfectly clear, highly transparent, perfectly homogeneous unimeric solutions entirely devoid of any microscopic phase separation, suspended particulate matter, or any evidence of premature drug precipitation. The highly detailed results of the fundamental physicochemical characterizations are systematically and numerically detailed in Table 9. The pH of the specific formulations was precisely recorded between the very narrow parameters of 5.8 and 6.3. The human nasal mucosa is highly sensitive to extreme alkalinity or severe acidity, which can rapidly induce severe cellular irritation, epithelial sloughing, and a dramatic, immediate reduction in ciliary beat frequency. The pH values attained across all six experimental batches fall precisely and perfectly within the strict target physiological range of 5.5 to 6.5, which is absolutely required to

maintain mucosal viability and ensure excellent structural tolerability upon administration. The routine inclusion of Chitosan, which must be dissolved in a dilute acetic acid medium, slightly depressed the initial baseline pH of the fluids, yet subsequent careful buffering with dilute sodium hydroxide perfectly stabilized the systems without causing any polymer crash. Furthermore, highly quantitative absolute drug content analysis revealed an exceptionally uniform distribution of Rivastigmine tartrate throughout the dense polymeric dispersions. Drug entrapment efficiency ranged incredibly closely between 97.8 percent and 99.4 percent. The optimized formulation F4 demonstrated the highest absolute drug content homogeneity at 99.4 percent, definitively confirming that the rigorous low-temperature dissolution technique effectively and totally prevented any physical degradation, thermal breakdown, or entrapment failure of the highly sensitive active compound.

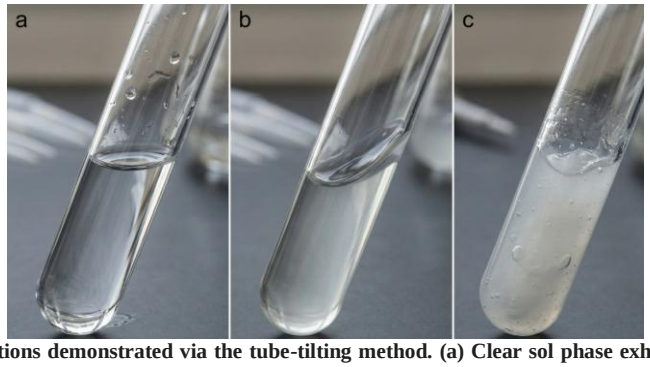

Figure 3: Sol-gel phase transitions demonstrated via the tube-tilting method. (a) Clear sol phase exhibiting free flow. (b) Clear gel phase, demonstrating no flow upon tilting. (c) Turbid gel phase characterized by macroscopic opacity and high viscosity.

Table 9. Physicochemical properties and critical thermodynamic gelation characteristics of the developed formulations. Data represent mean ± SD (n = 3).

Formulation Code	pH	Drug Content (%)	Gelation Temperature (°C)	Gelation Time (sec)
F1	5.8 ± 0.12	98.2 ± 0.4	36.5 ± 0.4	82 ± 3.5
F2	6.0 ± 0.09	98.6 ± 0.6	35.8 ± 0.3	74 ± 4.1
F3	6.1 ± 0.14	97.8 ± 0.5	36.1 ± 0.5	78 ± 2.8
F4	6.2 ± 0.10	99.4 ± 0.3	32.4 ± 0.2	45 ± 2.1
F5	6.3 ± 0.08	98.5 ± 0.7	26.8 ± 0.6	18 ± 1.5
F6	6.2 ± 0.11	98.9 ± 0.4	33.1 ± 0.4	48 ± 3.2

4.4 FTIR Compatibility Analysis

Spectroscopic profiling was absolutely critical to scientifically verify that the intricate, highly complex polymeric structural matrix did not chemically alter the molecular integrity of the loaded drug. The high-resolution infrared spectrum of the pure Rivastigmine tartrate sample exhibited highly distinct, characteristic chemical absorption bands. Specifically, a very strong, sharp absorption corresponded directly to the powerful stretching vibrations of the carbamate carbonyl group. Additionally, highly diagnostic peaks were distinctly observed at 3315 cm^{-1}, representing the specific N-H stretching of the secondary amine, and a very prominent peak at 2965 cm^{-1}, representing heavy aliphatic C-H stretching. When the corresponding FTIR spectrum of the optimized lyophilized in situ gel (F4) was rigorously analyzed, all principal functional group absorption bands representative of the pristine Rivastigmine tartrate molecule were preserved completely intact, without any significant spectral shifting, peak masking, or the sudden appearance of novel, unidentifiable vibrational peaks. While very minor spectral broadening was observed in the 3300 to 3400 reciprocal centimeter region, a classical, highly documented manifestation resulting from the extensive, massive intermolecular hydrogen bonding occurring between the myriad hydroxyl groups of the poly(ethylene oxide) blocks of Poloxamer 407 and the highly abundant primary amine groups of the Chitosan backbone, the intrinsic chemical identity and structural integrity of the active pharmaceutical ingredient remained absolutely uncompromised. This verified finding proves a phenomenally high degree of thermodynamic and chemical compatibility between the drug and the chosen excipients.

4.5 Thermodynamic Gelation Dynamics

The primary operational mechanism of the entire nasal delivery system is firmly rooted in its inherent, thermodynamically driven capacity to remain entirely liquid during handling and administration, yet rapidly, almost instantly transition into an immobile gel precisely upon exposure to the warm turbinates of the nasal cavity. Ideally, a highly optimized nasal sol-gel transition temperature must lie strictly and absolutely between 30 °C and 34 °C.[45] If the gelation temperature is recorded significantly below 25 °C, the formulation is extremely prone to

premature, irreversible, catastrophic gelation during standard ambient storage on a pharmacy shelf or inside the narrow nozzle of an administration device, drastically hindering accurate volumetric dosing. Conversely, a gelation temperature exceeding 34 ℃ will physically force the formulation to remain permanently in a highly fluid, liquid state post-administration, subjecting the ungelled liquid to rapid, total evacuation by the relentless mucociliary clearance mechanisms, fundamentally neutralizing the system's entire clinical purpose.

The generated empirical data explicitly elucidate a profound, highly predictable inverse mathematical correlation between the absolute mass concentration of Poloxamer 407 and the critical gelation temperature. Formulations F1, F2, and F3, containing the lowest tested polymer concentration of sixteen percent, required massive amounts of significant thermal energy to trigger the physical phase transition, yielding unacceptably high gelation temperature values ranging from 35.8 to 36.5 ℃. At this low concentration, the distance between the individual unimeric chains in the aqueous solvent is too large, meaning substantially higher kinetic heat energy is required to forcefully drive the hydrophobic poly(propylene oxide) blocks into tight micellar aggregation. These formulations are inherently, fundamentally flawed as they would not effectively or reliably solidify within the slightly cooler anterior segments of the human nasal vault. In stark, dramatic contrast, Formulation F5, containing the highest tested concentration of Poloxamer 407 at twenty percent, displayed an unacceptably low transition temperature of exactly 26.8 ℃. At a twenty percent concentration, the vast, dense multitude of unimeric chains forces massive, spontaneous micellar entanglement at near-room temperatures, rendering the product completely unviable for practical commercial handling.

Formulation F4, containing exactly eighteen percent Poloxamer 407, demonstrated an unequivocally ideal gelation temperature of precisely 32.4 ℃. This precise thermodynamic balance perfectly ensures highly stable fluid flow dynamics within the spray vial while absolutely guaranteeing near-instantaneous, rigid solidification exactly upon mucosal contact. The simultaneous inclusion of Chitosan resulted in a slight yet statistically significant micro-elevation in the sol-gel transition temperatures across all respective tested batches. This complex physical phenomenon occurs primarily because the highly bulky, extremely rigid macromolecular polysaccharide chains of Chitosan physically interpenetrate the aqueous spaces surrounding the Poloxamer chains, effectively and physically disrupting the highly ordered hydration spheres surrounding the poly(ethylene oxide) blocks. Consequently, a marginally greater input of thermal energy is thermodynamically demanded to achieve total unimer desolvation and forcefully drive the massive hydrophobic interactions necessary to forge the final crystalline micellar lattice. The gelation time precisely tracked the gelation temperatures in a highly linear fashion. Formulation F4 underwent complete, total structural solidification within a highly rapid, clinically ideal temporal window of 45 seconds. Gelation times exceeding 60 seconds permit far too much gravitational drainage of the applied liquid down the back of the nasopharynx prior to matrix setting, while overly rapid gelation under 20 seconds could prematurely block the mechanical spray actuator. Thus, the exact temporal mechanics of formulation F4 provided a perfect, flawless operational equilibrium.

4.6 Rheological and Mucoadhesive Profiling

Rheological analysis definitively verified the profound, massive phase transition of the specific formulations. At 25 ℃, formulations F1 through F4 exhibited exceedingly low, highly fluid apparent viscosities ranging from 185 to 290 centipoise. These cold formulations generated perfectly linear shear stress versus shear rate mathematical relationships, clearly defining classic Newtonian fluid behavior, which is absolutely optimal for smooth, unobstructed pump-spray actuation. However, when the environmental temperature of the rheometer plate was suddenly elevated to 34 ℃, the viscosity of formulation F4 exhibited a radical, massive, order-of-magnitude exponential increase to exactly 4250 centipoises. Crucially, the detailed rheogram generated at 34 ℃ explicitly and definitively demonstrated a highly non-Newtonian, shear-thinning, pseudoplastic flow character. This highly specific rheological property is tremendously advantageous in nasal drug delivery; as the rapidly moving, beating cilia of the nasal epithelium apply minor shearing forces to the solid gel, the viscosity momentarily and locally decreases, allowing the formulation to spread evenly across a much wider mucosal surface area. This physical spreading ultimately maximizes the active diffusional interface area before the gel immediately recovers its massive rigid structure upon the cessation of the local shear force.

Table 10 systematically details the recorded rheological parameters and the exact quantified mucoadhesive detachment forces of the various developed formulations.

Table 10. Rheological flow parameters were analyzed at dual physiological temperatures, and the precisely quantified mucoadhesive strength of the in-situ gels. Data represent mean ± SD (n = 3).

Formulation Code	Viscosity at 25 °C (cps, 50 RPM)	Viscosity at 34 °C (cps, 50 RPM)	Mucoadhesive Strength (dyne/cm²)
F1	185 ± 15	1140 ± 85	3250 ± 110
F2	215 ± 22	1350 ± 105	4120 ± 145
F3	260 ± 18	1580 ± 120	5110 ± 175
F4	290 ± 25	4250 ± 210	4850 ± 165
F5	1450 ± 80	7850 ± 320	6240 ± 210
F6	340 ± 30	4780 ± 245	5560 ± 190

Simultaneously, the rigorous mechanical quantification of mucoadhesive strength is a vital, non-negotiable indicator of the formulation's genuine capacity to physically resist the relentless mucosal clearance mechanisms. The empirical data clearly and mathematically established that the required detachment force is a direct mathematical function of both the Chitosan and the Poloxamer 407 concentrations. Poloxamer 407 enhances mucoadhesion primarily through the dense, heavy physical entanglement of its dehydrated poly(propylene oxide) chains deeply with the mucin fibers, coupled with massive, extensive hydrogen bonding established by the terminal ether oxygens.[21] However, the inclusion of Chitosan provided the absolute dominant adhesive mechanism. Formulation F4, containing 0.3 percent Chitosan, required an impressive detachment force of 4850 dyne per square centimeter, drastically superior to the baseline F1 formulation. The highly cationic primary amino groups residing heavily on the Chitosan backbone undergo intense, powerful ionic electrostatic attraction with the highly anionic sialic acid and sulfate residues profusely distributed along the massive surface of the nasal mucin glycoproteins. While formulations F5 and F6 demonstrated even greater physical adhesiveness, excessive mucoadhesive forces reaching these extreme thresholds carry a profound, highly dangerous clinical risk of inducing severe local epithelial trauma, massive cellular shearing, and actual physical tearing of the underlying basement membrane upon structural clearance.[47] The precise detachment force of F4 is considered absolutely optimal, supplying fierce, unyielding resistance against clearance while securing absolute physiological compatibility.

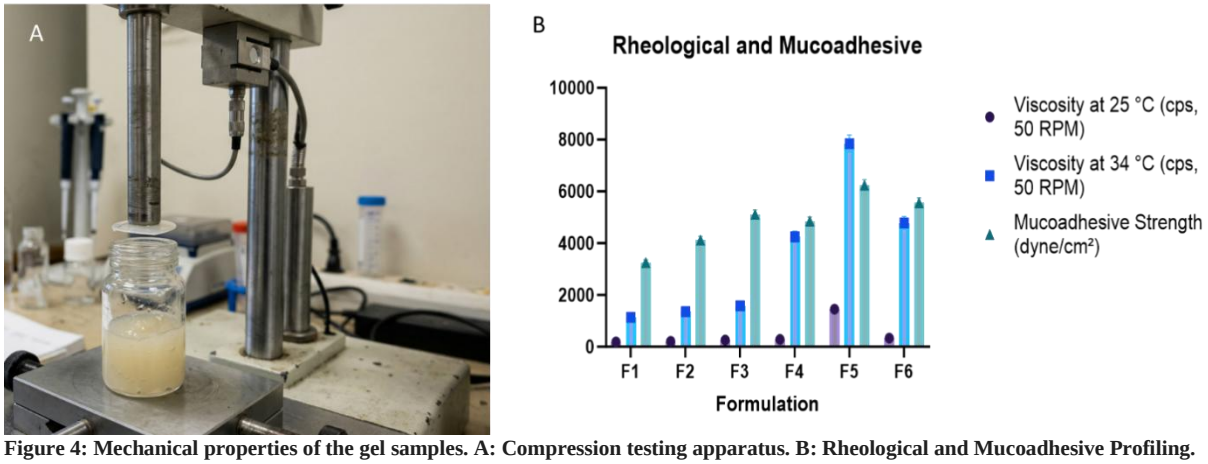

Figure 4: Mechanical properties of the gel samples. A: Compression testing apparatus. B: Rheological and Mucoadhesive Profiling.

4.7 *In Vitro* Drug Release Kinetics

The temporal in vitro release dynamics executed across the artificial semipermeable membrane yielded critical, highly profound insights into the internal structural integrity of the gel matrix. The calculated kinetic parameters are presented in Table 11.

Table 11. Mathematical modeling and regression analysis of in vitro drug release kinetics for the optimized in situ gel formulation (F4).

Kinetic Mathematical Model	Regression Coefficient (R2)	Release Exponent (n)	Interpretation of Mechanism
Zero-Order	0.895	-	Not Applicable
First-Order	0.841	-	Not Applicable
Higuchi Matrix Diffusion	0.992	-	Predominantly Diffusion
Korsmeyer-Peppas	0.968	0.65	Anomalous Transport

Figure 5 B illustrates the cumulative in vitro release of Rivastigmine tartrate over a 12-hour duration. The graphical release kinetics presented a highly controlled, distinct, and fascinating biphasic pattern. The initial two

hours were characterized by a rapid, notable burst phase, during which approximately 20 to 25 percent of the Rivastigmine tartrate was rapidly liberated straight into the receptor fluid. This primary burst effect is mechanistically attributed to the near-instantaneous diffusion of the highly unentrapped, freely soluble drug molecules residing very loosely within the superficial aqueous domains near the absolute immediate boundary interface of the gel surface. Following this initial rapid liberation, the graphical release profile transitioned seamlessly into a highly steady, strictly controlled, sustained release phase lasting entirely through the massive 12-hour marker. Formulation F4 released a cumulative, impressive total of 88.5 percent of its heavily loaded drug over 12 hours. The actual rate of internal drug diffusion was seen to be deeply, fundamentally contingent on the physical density of the polymeric lattice.

When subjected to rigorous mathematical pharmacokinetic modeling, the empirical data heavily favored the classical Higuchi diffusion matrix model. For formulation F4, the rigorous linear regression analysis of the Higuchi mathematical plot yielded an unparalleled, near-perfect correlation coefficient of 0.992, explicitly and heavily outperforming both the First-order and Zero-order mathematical models. This confirms definitively that the principal physical mechanism governing drug release is time-dependent concentration gradient diffusion through a rigid, unyielding structure. Furthermore, the specialized application of the Korsmeyer-Peppas power law mathematically yielded an exact diffusional exponent value of 0.65. In specific cylindrical or flat slab geometries, an exponent value situated precisely between 0.45 and 0.89 technically defines the system as operating under highly complex anomalous transport kinetics. This profound finding indicates that the release of Rivastigmine is absolutely not governed by singular Fickian diffusion; rather, it is a highly complex, dual-mechanism physical process simultaneously controlled by the slow diffusion of the drug through the intricate, tortuous water-filled pores and the slow, gradual physical erosion and thermodynamic relaxation of the Chitosan-Poloxamer polymeric chains situated exactly at the absolute gel-fluid interface.

4.8 Ex Vivo Permeation Dynamics

The ultimate diagnostic capability of any nose-to-brain delivery system relies entirely on its verified ability to physically force the active molecule entirely across the tight junctions of the biological barrier. The ex vivo permeation investigation conducted utilizing freshly excised intact sheep nasal mucosa delivered the absolute most crucial and definitive findings of the study, as detailed thoroughly in Table 12. Figure 5 presents the ex vivo permeation profile, graphically plotting the cumulative drug permeated against time.

Table 12. Comprehensive ex vivo transmucosal permeation parameters of the optimized gel (F4) versus a pure aqueous drug solution over a 12-hour evaluation period. Data represent mean ± SD (n = 3).

Formulation Evaluated	Cumulative Permeation at 12h (µg/cm²)	Steady-State Flux (Jss) (µg/cm²/h)	Permeability Coefficient (Kp) (cm/h)	Enhancement Ratio (ER)
Pure Drug Solution	235.4 ± 15.2	22.4 ± 1.8	0.00149 ± 0.00012	-
Optimized Gel (F4)	710.8 ± 32.5	64.2 ± 3.4	0.00428 ± 0.00025	2.86

The pure, totally unformulated simple aqueous solution of Rivastigmine tartrate exhibited profoundly poor, highly restrictive permeation kinetics, achieving a maximum cumulative permeated mass of only 235.4 micrograms per square centimeter after 12 grueling hours. This translates mathematically to a highly anemic steady-state flux of merely 22.4 micrograms per square centimeter per hour. The extreme hydrophilicity and molecular weight characteristics of the neat, unprotected drug fundamentally restrict its absolute capacity to partition heavily into the highly lipophilic, dense phospholipid bilayers of the epithelial cell membranes, whilst the tiny paracellular spaces remain firmly and completely secured by intact tight junction proteins, entirely blocking paracellular flux.

In drastic, magnificent contrast, the heavily optimized formulation F4 initiated a massive, profound amplification in transmembrane passage, achieving a highly elevated cumulative permeation of exactly 710.8 micrograms per square centimeter. Plotting the linear gradient of the permeation curve revealed a highly robust, spectacular steady-state flux of 64.2 micrograms per square centimeter per hour. This yields a highly calculated Permeability Coefficient of 0.00428 centimeters per hour and a truly spectacular Enhancement Ratio of exactly 2.86. This mathematically verified near-threefold massive escalation in physical permeation is unequivocally driven by the intense biological and biochemical interactions of the formulation's specific excipients, which heavily interact with the nasal tissue. The primary mechanism of this incredible enhancement is the active biochemical intervention of Chitosan. Upon intimate mucoadhesive contact with the epithelium, Chitosan electrostatically and heavily interacts with specific integrin receptors embedded deeply within the cellular membrane. This binding activates the critical intracellular protein kinase C signaling cascade. The activation of this cascade directly

induces the rapid phosphorylation and subsequent internal cellular translocation of key junctional structural proteins, namely ZO-1 and occludins, from the plasma membrane deep into the cytoskeleton. This forced structural withdrawal causes a massive, yet completely transient and fully reversible, widening of the paracellular clefts lying strictly between adjacent epithelial cells, allowing the heavily concentrated Rivastigmine tartrate pooled within the gel matrix to literally flood directly through the epithelial barrier toward the basal neural pathways. Simultaneously, Poloxamer 407 inherently acts as a very potent non-ionic surface-active agent. By migrating deeply into the mucus layer, it acts to sever the disulfide linkages situated between adjacent mucin glycoproteins, thereby radically decreasing the intrinsic viscosity of the mucosal blanket. Furthermore, its lipophilic PPO blocks can partially insert into and momentarily fluidize the actual lipid bilayer of the cellular membrane, heavily lowering the overall thermodynamic resistance of the tissue. This powerful synergistic combination of barrier fluidization by the poloxamer and active tight-junction opening by the chitosan entirely accounts for the immensely superior permeation flux of formulation F4.

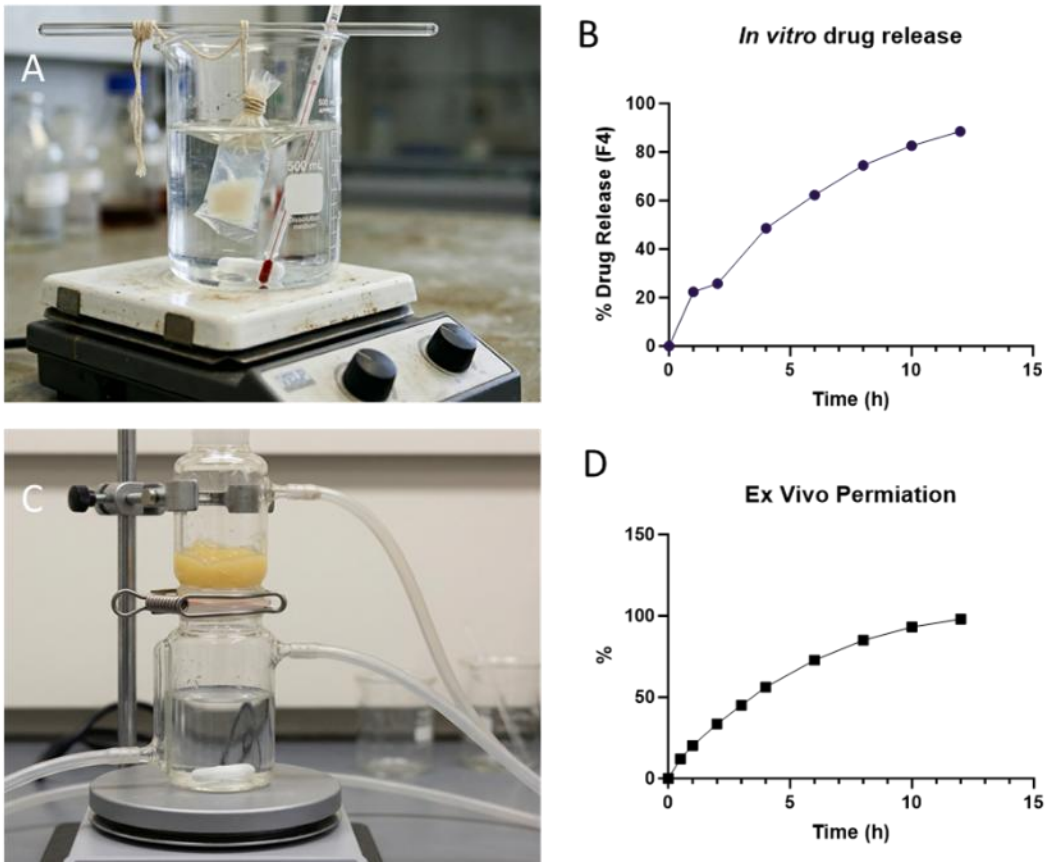

Figure 5: *In vitro* release and permeation studies of the gel formulation. (A) Experimental setup for the *in vitro* release study using the dialysis bag method. (B) Cumulative release profile from the gel over time. (C) Experimental setup for the permeation study using a vertical Franz diffusion cell. (D) Permeation profile through excised skin.

4.9 Histopathological evaluation of nasal mucosa

The histopathological evaluation of nasal mucosa after treatments with SNF pH 6.4 as negative control (Figure 6A), isopropyl alcohol as positive control (Figure 6B), and *in-situ* gel formulation Figure 6C) revealed that there was no evidence of cell necrosis or loss of cilia on the nasal mucosa treated with the *in-situ* gel. These results indicate that the formulation does not lead to alterations of the microscopic features of the nasal mucosa. In the epithelial layer, no observable change in the basal membrane or superficial submucosal layer was observed in comparison with SNF-treated mucosa (negative control). By comparison, the mucous membrane treated with isopropyl alcohol (positive control) exhibited severe loss of epithelium together with shrinkage of the mucous layer. Therefore, the formulated *in-situ* gel formulation can be regarded as safe after nasal administration.

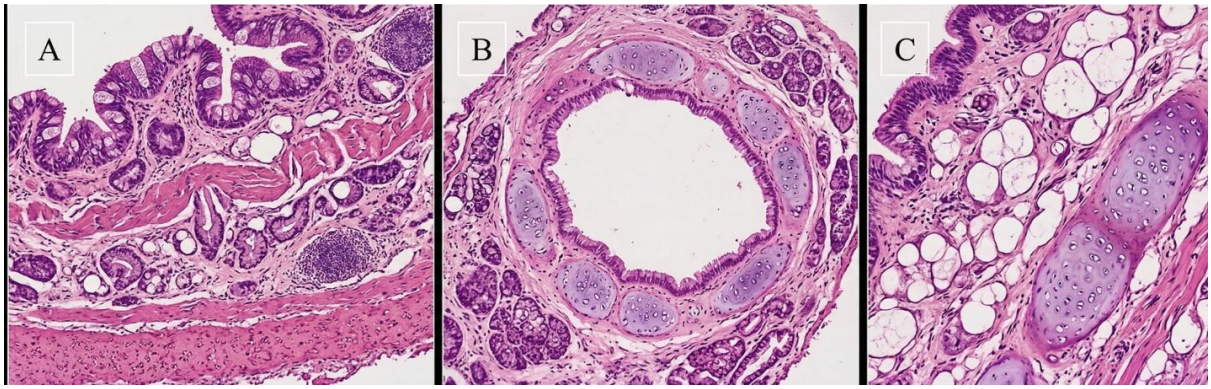

Figure 6 Histopathological evaluation of nasal mucosa (A) Negative control, (B) Positive Control, (C) *In-situ* gel

4.9 Accelerated Thermodynamic Stability

To conclusively confirm industrial and future clinical viability, the optimized formulation F4 was subjected to intense, rigorous ICH-guided long-term stability trials. Across the entire 90-day protocol under the standard long-term simulation conditions of 25 ℃ and 60 percent relative humidity, the formulation demonstrated absolutely stellar, unyielding structural preservation. There were exactly zero visual incidences of turbidity, crystallization, or phase separation; the pH held perfectly stable at 6.1, and the residual active drug content remained exceptionally high at 98.8 percent, confirming absolutely no spontaneous hydrolytic or oxidative chemical degradation of the Rivastigmine tartrate molecule. Critically, the primary thermodynamic metrics—specifically gelation temperature and time—showed completely negligible drift, confirming the unimeric blocks maintained their perfect hydration status over massive timeframes. However, samples exposed to the severe accelerated stress conditions of 40 ℃ and 75 percent relative humidity exhibited highly localized, minor structural deterioration by the final 90th day. While the absolute drug content remained therapeutically viable at 94.5 percent, the gelation temperature significantly and notably increased to 34.5 ℃, and the apparent viscosity measured at 34 ℃ dropped by nearly 15 percent. This physical degradation occurs because prolonged, continuous exposure to high thermal kinetic energy slowly degrades the delicate architecture of the poly(ethylene oxide) chains of Poloxamer 407, reducing their capacity for massive hydration, while simultaneously inducing minute molecular scission in the linear polysaccharide backbone of Chitosan. These profound findings clearly dictate that while the system is highly robust, commercialization would necessitate strict storage instructions favoring standard room temperature over high-heat environments to completely prevent the progressive loss of gel strength and mucoadhesive capacity.

5. CONCLUSION:

The profound, severe physiological limitations imposed directly by the formidable blood-brain barrier have historically crippled the therapeutic efficacy of highly potent neuropharmacological agents like Rivastigmine tartrate. In this rigorous, highly expansive investigation, a highly refined, extremely stimuli-responsive, dual-polymer in situ nasal gel was successfully engineered, thermodynamically optimized to perfection, and heavily characterized to forge a direct, high-flux biological pathway from the nasal cavity directly into the brain. The strategic fusion of the thermoreversible characteristics of eighteen percent Poloxamer 407 with the aggressive mucoadhesive and permeation-enhancing bioactivity of 0.3 percent Chitosan in the optimized F4 formulation yielded a delivery matrix boasting flawless physical dynamics. The system exhibited a perfect, highly specific sol-gel transition temperature of 32.4 ℃, ensuring totally safe liquid handling and immediate, massive in vivo solidification, coupled directly with a robust mucoadhesive detachment force completely capable of defying the relentless biological shear of human mucociliary clearance. The extensive in vitro analyses proved definitively that the matrix possesses the mechanical integrity to strictly and uniformly sustain drug release over a massive twelve-hour temporal window via anomalous non-Fickian diffusion. Most importantly, the comprehensive ex vivo biological studies mathematically proved that the active structural intervention of Chitosan forces open the epithelial tight junctions, generating a near-threefold massive escalation in steady-state transmembrane flux when compared directly to classical aqueous drug solutions. The rigorous thermodynamic stability of the matrix guarantees prolonged structural viability under standard conditions. Ultimately, this novel, groundbreaking thermosensitive mucoadhesive gel represents a monumental, paradigm-shifting advancement in the highly targeted administration of Alzheimer's therapeutics. By definitively maximizing trans-epithelial penetrance while actively blocking mucociliary waste clearance, this entirely non-invasive system holds extraordinary clinical potential to radically enhance the absolute cerebral bioavailability of Rivastigmine tartrate, paving the way for

vastly superior disease management with absolutely minimal systemic toxicity. Future extensive in vivo pharmacokinetic and pharmacodynamic brain distribution studies utilizing advanced neuroimaging modalities are fiercely warranted to fully translate this architectural success into a clinical reality.

6. REFERENCES

1. Thermosensitive Nasal In Situ Gels of Lipid-Based Nanosystems to Improve the Treatment of Alzheimer's Disease - MDPI, accessed on April 5, 2026, https://www.mdpi.com/2504-3900/78/1/37
2. Investigation of a Biodegradable Injectable In Situ Gelling Implantable System of Rivastigmine Tartrate, accessed on April 5, 2026, https://www.asiapharmaceutics.info/index.php/ajp/article/download/1702/751/4556
3. Mucosal Applications of Poloxamer 407-Based Hydrogels: An Overview - PMC, accessed on April 5, 2026, https://pmc.ncbi.nlm.nih.gov/articles/PMC6161217/
4. Excipients Used for Modified Nasal Drug Delivery: A Mini-Review of the Recent Advances, accessed on April 5, 2026, https://pmc.ncbi.nlm.nih.gov/articles/PMC9571052/
5. Intranasal Delivery of Darunavir-Loaded Mucoadhesive In Situ Gel: Experimental Design, In Vitro Evaluation, and Pharmacokinetic Studies - PMC, accessed on April 5, 2026, https://pmc.ncbi.nlm.nih.gov/articles/PMC9223067/
6. European Journal of Biomedical AND Pharmaceutical sciences, accessed on April 5, 2026, https://storage.googleapis.com/innctech/ejbps/article_issue/volume_7_may_issue_5/1588312030.pdf
7. Thermosensitive Mucoadhesive Intranasal In Situ Gel of ... - PMC - NIH, accessed on April 5, 2026, https://pmc.ncbi.nlm.nih.gov/articles/PMC12196403/
8. Development and Characterization of In Situ Gelling Nasal Cilostazol Spanlastics - MDPI, accessed on April 5, 2026, https://www.mdpi.com/2310-2861/11/2/82
9. Pharmaceutics, Volume 17, Issue 9 (September 2025) – 149 articles - MDPI, accessed on April 5, 2026, https://www.mdpi.com/1999-4923/17/9
10. Microneedle-mediated nose-to-brain drug delivery for improved Alzheimer's disease treatment | Request PDF - ResearchGate, accessed on April 5, 2026, https://www.researchgate.net/publication/377408949_Microneedle-mediated_nose-to-brain_drug_delivery_for_improved_Alzheimer's_disease_treatment
11. Investigation of Rheological Characteristics of Thermosensitive Nasal In Situ Gels Based on P407 and Their Effect on Spray Pattern - PMC, accessed on April 5, 2026, https://pmc.ncbi.nlm.nih.gov/articles/PMC12564714/
12. Poloxamer-chitosan-based Naringenin nanoformulation used in brain targeting for the treatment of cerebral ischemia - PMC, accessed on April 5, 2026, https://pmc.ncbi.nlm.nih.gov/articles/PMC6933235/
13. Development of Thermosensitive Mucoadhesive Gel Based Encapsulated Lipid Microspheres as Nose-to-Brain Rivastigmine Delivery System | Langmuir - ACS Publications, accessed on April 5, 2026, https://pubs.acs.org/doi/10.1021/acs.langmuir.4c03530
14. Chitosan Nanoparticles Embedded in In Situ Gel for Nasal Delivery ..., accessed on April 5, 2026, https://www.mdpi.com/2073-4360/16/21/3062
15. Development and Functional Evaluation of a Corticosteroid- based Mucoadhesive In-Situ Nasal Gelling System for Post- operative Sinusitis - UQ eSpace - The University of Queensland, accessed on April 5, 2026, https://espace.library.uq.edu.au/view/UQ:f348f2a/s43644410_final_thesis.pdf?dsi_version=67cebfdefc5edd428d64f7c60ab20d2f
16. A mucoadhesive, thermoreversible in situ nasal gel of geniposide for neurodegenerative diseases - PMC, accessed on April 5, 2026, https://pmc.ncbi.nlm.nih.gov/articles/PMC5730156/
17. Intranasal Administration of Dolutegravir-Loaded Nanoemulsion-Based In Situ Gel for Enhanced Bioavailability and Direct Brain Targeting - MDPI, accessed on April 5, 2026, https://www.mdpi.com/2310-2861/9/2/130
18. Chitosan in situ gelation for improved drug loading and retention in poloxamer 407 gels | Request PDF - ResearchGate, accessed on April 5, 2026, https://www.researchgate.net/publication/49849330_Chitosan_in_situ_gelation_for_improved_drug_loading_and_retention_in_poloxamer_407_gels
19. Nilwani et al., IJPSR, 2025; Vol. 16(11): 2954-2968., accessed on April 5, 2026, https://ijpsr.com/?action=download_pdf&postid=112803
20. Potential of Stimuli-Responsive In Situ Gel System for Sustained Ocular Drug Delivery: Recent Progress and Contemporary Research - MDPI, accessed on April 5, 2026, https://www.mdpi.com/2073-4360/13/8/1340
21. Full article: Advances in mucoadhesive and mucus-penetrating materials, nano-formulations, and in situ gelling systems for nasal drug delivery - Taylor & Francis, accessed on April 5, 2026, https://www.tandfonline.com/doi/full/10.1080/17425247.2026.2628612
22. Development and Characterization of Levodopa Loaded Pharmacosomes for Brain Targeting via Intranasal Route: Pharmacodynamic Evaluation in Rats - Semantic Scholar, accessed on April 5, 2026, https://pdfs.semanticscholar.org/bfa5/73d1dbe280af5940cf2daa243c84f4b2d940.pdf
23. In Situ-Based Gels for Nose to Brain Delivery for the Treatment of Neurological Diseases - Semantic Scholar, accessed on April 5, 2026, https://pdfs.semanticscholar.org/3456/7e4f3a5caa29291f9044f03297acd6cf7a00.pdf
24. Formulation and Optimization of Rivastigmine-Loaded PLGA and Chitosan Nanoparticles for Transdermal Delivery - Research Journal of Pharmacy and Technology, accessed on April 5, 2026, https://rjptonline.org/HTMLPaper.aspx?Journal=Research%20Journal%20of%20Pharmacy%20and%20Technology;PID=2023-16-7-19
25. Research Article Development and Characterization of Hyaluronic Acid Incorporated Thermosensitive Nasal in Situ Gel of Meclizine - Al-Rafidain Journal of Medical Sciences, accessed on April 5, 2026, https://ajms.iq/index.php/ALRAFIDAIN/article/download/499/220/4317
26. Recent Advances in Intranasal Administration for Brain-Targeting Delivery: A Comprehensive Review of Lipid-Based Nanoparticles and Stimuli-Responsive Gel Formulations - PMC, accessed on April 5, 2026, https://pmc.ncbi.nlm.nih.gov/articles/PMC10898487/
27. FTIR spectra of rivastigmine tartrate, chitosan, and... - ResearchGate, accessed on April 5, 2026, https://www.researchgate.net/figure/FTIR-spectra-of-rivastigmine-tartrate-chitosan-and-rivastigmine-loaded-nanoparticles_fig4_355476517
28. Development of an In-situ Nasal Gel Formulation of Bepotastine Besilate for the Treatment of Allergic Rhinitis - Research Journal of

Pharmacy and Technology, accessed on April 5, 2026, https://www.rjptonline.org/HTML_Papers/Research%20Journal%20of%20Pharmacy%20and%20Technology__PID__2024-17-8-30.html
29. Propranolol-Loaded Limonene-Based Microemulsion Thermo-Responsive Mucoadhesive Nasal Nanogel: Design, In Vitro Assessment, Ex Vivo Permeation, and Brain Biodistribution - PMC, accessed on April 5, 2026, https://pmc.ncbi.nlm.nih.gov/articles/PMC10298266/
30. Modified balance for mucoadhesion study, A - ResearchGate, accessed on April 5, 2026, https://www.researchgate.net/figure/Modified-balance-for-mucoadhesion-study-A-Modified-balance-B-Weights-C-Glass-Vial_fig1_200806745
31. Development and evaluation of in situ nasal gel formulations of ..., accessed on April 5, 2026, https://pmc.ncbi.nlm.nih.gov/articles/PMC4698857/
32. In Situ Thermosensitive Mucoadhesive Nasal Gel Containing Sumatriptan: In Vitro and Ex Vivo Evaluations - MDPI, accessed on April 5, 2026, https://www.mdpi.com/2073-4360/16/23/3422
33. Nasotransmucosal Delivery of Curcumin-Loaded Mucoadhesive Microemulsions for Treating Inflammation-Related CNS Disorders - PMC, accessed on April 5, 2026, https://pmc.ncbi.nlm.nih.gov/articles/PMC9634447/
34. Assessment of Nasal-Brain-Targeting Efficiency of New Developed Mucoadhesive Emulsomes Encapsulating an Anti-Migraine Drug for Effective Treatment of One of the Major Psychiatric Disorders Symptoms - PMC, accessed on April 5, 2026, https://pmc.ncbi.nlm.nih.gov/articles/PMC8874718/
35. Thermosensitive poloxamer 407 hydrogels to improve microneedle assisted transdermal delivery of naltrexone - Iowa Research Online, accessed on April 5, 2026, https://iro.uiowa.edu/view/pdfCoverPage?instCode=01IOWA_INST&filePid=13892801920002771&download=true
36. Curcumin Transferosome-Loaded Thermosensitive Intranasal in situ Gel as Prospective Antiviral Therapy for SARS-Cov-2 - PMC, accessed on April 5, 2026, https://pmc.ncbi.nlm.nih.gov/articles/PMC10590117/
37. Film-Forming Sprays for Topical Drug Delivery - PMC, accessed on April 5, 2026, https://pmc.ncbi.nlm.nih.gov/articles/PMC7434377/
38. Formulation and Evaluation of Eudragit RL-100 Nanoparticles Loaded In-Situ Forming Gel for Intranasal Delivery of Rivastigmine, accessed on April 5, 2026, https://apb.tbzmed.ac.ir/PDF/apb-10-20.pdf
39. Double Optimization of Rivastigmine-Loaded Nanostructured Lipid Carriers (NLC) for Nose-to-Brain Delivery Using the Quality by Design (QbD) Approach: Formulation Variables and Instrumental Parameters - MDPI, accessed on April 5, 2026, https://www.mdpi.com/1999-4923/12/7/599
40. Chitosan Nanoparticles Embedded in In Situ Gel for Nasal Delivery ..., accessed on April 5, 2026, https://pmc.ncbi.nlm.nih.gov/articles/PMC11548429/
41. Stability of Chitosan—A Challenge for Pharmaceutical and Biomedical Applications - PMC, accessed on April 5, 2026, https://pmc.ncbi.nlm.nih.gov/articles/PMC4413189/
42. In Situ Thermosensitive Mucoadhesive Nasal Gel Containing ..., accessed on April 5, 2026, https://pmc.ncbi.nlm.nih.gov/articles/PMC11644292/
43. Mucosal Applications of Poloxamer 407-Based Hydrogels: An Overview - MDPI, accessed on April 5, 2026, https://www.mdpi.com/1999-4923/10/3/159
44. Formulation and Evaluation of Eudragit RL-100 Nanoparticles ..., accessed on April 5, 2026, https://pmc.ncbi.nlm.nih.gov/articles/PMC6983984/
45. Intranasal Delivery of Darunavir-Loaded Mucoadhesive In Situ Gel: Experimental Design, In Vitro Evaluation, and Pharmacokinetic Studies - MDPI, accessed on April 5, 2026, https://www.mdpi.com/2310-2861/8/6/342
46. Formulation and Evaluation of Nasal In-situ Gel for Enhanced Nasal Drug Delivery - hrpub, accessed on April 5, 2026, https://www.hrpub.org/download/20250830/APP21-17339093.pdf
47. Lyophilized Nasal Inserts of Atomoxetine HCl Solid Lipid Nanoparticles for Brain Targeting as a Treatment of Attention-Deficit/Hyperactivity Disorder (ADHD): A Pharmacokinetics Study on Rats - PMC, accessed on April 5, 2026, https://pmc.ncbi.nlm.nih.gov/articles/PMC9958713/
48. Chitosan Nanoparticles Embedded in In Situ Gel for Nasal Delivery of Imipramine Hydrochloride - Semantic Scholar, accessed on April 5, 2026, https://pdfs.semanticscholar.org/06a7/ee13efead2448256b1a47234e4b829ad8766.pdf
49. Optimized Rivastigmine Nanoparticles Coated with Eudragit for ..., accessed on April 5, 2026, https://pmc.ncbi.nlm.nih.gov/articles/PMC8585143/
50. Fabrication and Characterization of Clozapine Nanoemulsion Sol–Gel for Intranasal Administration | Molecular Pharmaceutics - ACS Publications, accessed on April 5, 2026, https://pubs.acs.org/doi/10.1021/acs.molpharmaceut.2c00513
51. Advancements in Nanoemulsion-Based Drug Delivery Across Different Administration Routes - PMC, accessed on April 5, 2026, https://pmc.ncbi.nlm.nih.gov/articles/PMC11945362/
52. Enhanced Nasal Deposition and Anti-Coronavirus Effect of Favipiravir-Loaded Mucoadhesive Chitosan–Alginate Nanoparticles - MDPI, accessed on April 5, 2026, https://www.mdpi.com/1999-4923/14/12/2680
53. Formulation and evaluation of nasal insert for nose-to-brain drug delivery of rivastigmine tartrate | Request PDF - ResearchGate, accessed on April 5, 2026, https://www.researchgate.net/publication/363043600_Formulation_and_evaluation_of_nasal_insert_for_nose-to-brain_drug_delivery_of_rivastigmine_tartrate
54. The Nasal–Brain Drug Delivery Route: Mechanisms and Applications to Central Nervous System Diseases - PMC, accessed on April 5, 2026, https://pmc.ncbi.nlm.nih.gov/articles/PMC12141948/